Inflammation Research (2019) 68:643–654
https://doi.org/10.1007/s00011-019-01246-8

Inflammation Research

ORIGINAL RESEARCH PAPER

microRNA-520c-3p suppresses NLRP3 inflammasome activation and inflammatory cascade in preeclampsia by downregulating NLRP3

Zhaochun Liu[1] · Xia Zhao[1] · HongYing Shan[1] · Huan Gao[1] · Ping Wang[1]

Received: 18 November 2018 / Revised: 22 April 2019 / Accepted: 6 May 2019 / Published online: 30 May 2019

Abstract

Background The pathogenesis of preeclampsia (PE) is suggested to be a consequence of inflammation. Previously conducted investigations on nod-like receptor pyrin domain-containing 3 (NLRP3) have shed light to its crucial role in PE. Furthermore, microRNA-520c-3p (miR-520c-3p) is observed to be implicated in inflammation. Therefore, the current study aimed to explore the role of miR-520c-3p in inflammatory cascade of PE by targeting NLRP3.

Methods Microarray analyses were performed to screen differentially expressed genes associated with PE, and the potential relationship between miR-520c-3p and NLRP3 was analyzed. PE and normal placenta tissues were collected to determine the levels of inflammatory cytokines (IL-18, IL-33, IL-1β, IL-10, and TNF-α), miR-520c-3p and NLRP3. Hypoxic HTR8/SVneo cells were transfected with oe-NLRP3, si-NLRP3 or miR-520c-3p mimic to elucidate the functional role of NLRP3 or miR-520c-3p in the inflammatory cascade in PE, followed by the evaluation of levels of inflammatory cytokines and NLRP3 inflammasomes (NLRP3, ASC and caspase-1). Additionally, the HTR8/SVneo cell migration and invasion were evaluated.

Results An upregulation of NLRP3, IL-18, IL-1β and TNF-α, and downregulation of miR-520c-3p, IL-33 and IL-10 were observed in PE placenta tissues. NLRP3 was found to be a target gene of miR-520c-3p. HTR8/SVneo cells after hypoxia transfected with si-NLRP3 or miR-520c-3p mimic exhibited decreased levels of inflammatory cytokines and NLRP3 inflammasomes, in addition to increased IL-10 and IL-33 levels. Moreover, enhanced migration and invasion abilities were observed in cells transfected with si-NLRP3.

Conclusion Collectively, miR-520c-3p could potentially inhibit NLRP3 inflammasome activation and inflammatory cascade in PE by downregulating NLRP3, highlighting the potential of miR-520c-3p as a therapeutic target for PE treatment.

Keywords microRNA-520c-3p · NLRP3 inflammasomes · Preeclampsia · Inflammatory cascade

Background

Preeclampsia (PE) is a placenta-induced inflammatory disorder accompanied by maternal and fetal morbidity and mortality, and the pathogenesis of PE shares an association with inflammation [1]. Approximately 3–5% of all pregnancies are affected by PE, accounting for more than 60,000 cases of maternal annual deaths [2]. Currently, the only curative treatment of PE remains to be the removal of placenta through delivery [3]. Known factors that are associated with the development and progression of PE include insufficient trophoblast invasion and poor remodeling of uterine spiral arteries [4]. Previously, vascular abnormalities and inflammation have been found in placentas from women with PE when compared to healthy pregnancies, highlighting the crucial role played by inflammation in this pregnancy complication [5]. Moreover, the existence of imbalanced inflammatory cytokine production such as pro-inflammatory cytokines including tumor necrosis factor alpha (TNF-α) and anti-inflammatory cytokines including interleukin (IL)-10 during the placental-decidual interface is reflected in maternal and umbilical circulation [6]. Therefore, it is trivial to seek out potential therapeutic approaches for an effective treatment of inflammation in PE.

Responsible Editor: John Di Battista.

✉ Xia Zhao
zhaoxia_1115@126.com

[1] Obstetrics Department, The First Affiliated Hospital of the Medical College, Shihezi University, No. 107, North 2nd Road, Shihezi 832008, The Xinjiang Uygur Autonomous Region, People's Republic of China

Nod-like receptor pyrin domain-containing 3 (NLRP3) inflammasome, which comprises NLRP3, apoptotic speck-like protein containing a CARD domain (ASC) and caspase-1, has been previously demonstrated to be involved in various inflammatory diseases such as atherosclerosis [7]. A former study further demonstrated increased expression patterns of NLRP3 inflammasomes in placentas from women with PE, suggesting an association between activated NLRP3 inflammasomes and aggravated inflammatory states [8]. NLRP3 forms a major member of the NLRP3 inflammasomes, whose mutation results in enhancement of NLRP3 inflammasome activity and IL-1β over-production [9]. According to an online prediction software and dual-luciferase reporter gene assay, NLRP3 was confirmed to be a target gene of microRNA-520c-3p (miR-520c-3p). Furthermore, numerous microRNAs (miRNAs) have been documented to function as regulators of immune and inflammatory responses, indicating the existence of close association between dysregulated expression of specific miRNAs and activated inflammatory responses [10]. Specifically, miR-520/373 family was demonstrated to act as a tumor suppressor for estrogen receptor-negative breast cancer by means of bridging the NF-κB and TGF-β pathways, thus promoting the interaction among tumor progression, metastasis and inflammation [11]. In addition, miR-520c has been reported to be upregulated eightfold in periodontitis compared to healthy gingiva, indicating its potential participant role in chronic periodontitis inflammation [12]. In addition, enriched expression of miR-520c-3p is revealed in trophoblast, while it is downregulated by hypoxia [13]. Therefore, we hypothesized that miR-520c-3p could be involved in NLRP3 inflammasomes and inflammatory cascade in HTR8/SVneo cells after hypoxia by targeting NLRP3. The current study aims to define the major role and explore potential mechanism of miR-520c-3p/NLRP3 in PE, hoping to uncover a promising therapeutic approach for PE treatment.

Materials and methods

Ethic statement

The current study was approved by the Ethics Committee of the First Affiliated Hospital of the Medical College, Shihezi University (AF/SC-07/01.1). Signed informed consents were obtained from all participating patients prior to enrollment into the study.

Microarray-based analysis

The Gene Expression Omnibus (GEO) database (https://www.ncbi.nlm.nih.gov/geo/) was used to retrieve the gene expression profiles and probe annotation files of GSE96983 datasets, which are comprised of four cases of normal placenta samples and three cases of PE placenta samples. The Affy package of R language was applied for both pre-processing and standardization of the gene expression data, and the limma package was adopted for screening the differentially expressed genes (adj. *p* Val referred to a corrected *p* value). The screening threshold for differentially expressed genes was set as |LogFoldChange| > 2 and adj. *p* val < 0.05, and subsequently, a heat map was plotted.

Study subjects

A total of 30 cases of PE placenta tissues (PE group) and 30 cases of normal placenta tissues (control group) hospitalized at the First Affiliated Hospital of the Medical College, Shihezi University, between September 2016 and September 2017 were enrolled in the current study. The diagnostic criteria were applied following the parameters of a previous study [14]. Specifically, all included patients underwent termination of pregnancy via cesarean section with epidural anesthesia. Patients presenting with hypertension, heart disease, diabetes, thyroid disease, kidney disease, and other complications that may lead to hypoxic changes were excluded [14]. After delivery of the placenta, the placental tissues with a size of about 1 cm × 1 cm × 1 cm were cut around the umbilical cord in the central region of the maternal surface of placenta (avoiding organization, calcification or hemorrhagic foci). All obtained tissues were frozen in liquid nitrogen within 20 min after the separation and stored at − 80 °C for further use. The clinical data of patients hospitalized between September 2016 and September 2017 in the PE group and the control group are shown in Table 1.

Enzyme-linked immunosorbent assay (ELISA)

The placenta specimens were thawed, and 500 mg of placenta tissues was rinsed twice with 400 mL of Tris–Cl buffer with the excess liquid removed using filter paper. Next, the

Table 1 The clinical data of patients in the control and PE group

Indicator	Control	PE
Case	30	30
Age	28.67 ± 2.78	27.07 ± 2.53
Gestational week	37.90 ± 0.92	36.90 ± 0.96
BMI (kg/m^2)	24.86 ± 1.94	24.18 ± 1.63
MABP (mmHg)	97.76 ± 2.94	119.87 ± 6.04
24-h urinary protein (g)	0.09 ± 0.02	2.16 ± 0.17
Neonatal weight (g)	3364.82 ± 198.44	2802.33 ± 231.11
PLW (g)	653.24 ± 34.17	459.37 ± 38.67

BMI body mass index, *MABP* mean arterial blood pressure, *PLW* placental weight, *PE* preeclampsia

placenta tissues were placed in 2 mL of Tris–Cl buffer containing protease inhibitor and homogenized for 60 s using an ultrasonic-homogenization machine. Then, the tissues were centrifuged at 7246×*g* for 20 min at 4 °C with the supernatant collected and preserved at a − 70 °C freezer for subsequent use. The levels of IL-18, IL-33, IL-1β, caspase-1, IL-10, and TNF-α were, respectively, detected according to the instructions of the following ELISA kits: IL-18 (E03641, Shanghai Walan Biotech Co., Ltd., Shanghai, China), IL-33 (KL01534, Shanghai Kanglang Biological Co., Ltd., Shanghai, China), IL-1β (583311-96, AmyJet Scientific, Wuhan, Hubei, China), IL-10 (ab46034, Abcam, Cambridge, MA, USA), caspase-1 (C101, Beyotime Biotechnology Co., Ltd., Shanghai, China), and TNF-α (K1052-100, AmyJet Scientific, Wuhan, Hubei, China).

Immunohistochemistry

Subsequently, 3–5-μm placenta tissues from each group were extracted, attached to slides treated with polylysine, and then baked at 65 °C for 4.5 h, dewaxed twice with xylene (3 min/time), dehydrated once in gradient alcohol for 2 min, and finally washed under water for 2 min. Next, the slides were immersed in 3% methanol H_2O_2 for 20 min, and washed with distilled water for 2 min, followed by 3-min rinsing using 0.1 M phosphate buffer saline (PBS). Then, the slides were water-bath repaired in an antigen repair solution, and the temperature was lowered for 3–5 min after boiling and cooled down under running water. Following cooling, the slides were blocked with normal goat serum blocking solution (C-0005, Shanghai Haoran Biotechnology Co., Ltd., Shanghai, China) at room temperature for 30 min with the excess liquid being dried. Next, the slides were incubated with the primary antibody rabbit polyclonal antibody to NLRP3 (dilution ratio of 1:500, ab214185, Abcam Inc., Cambridge, MA, USA) overnight at 4 °C, followed by three 0.1 M PBS rinses (5 min/time). On the following day, the slides were further incubated with the secondary antibody anti-rabbit immunoglobulin G (IgG) (dilution ratio of 1:1000, ab6721, Abcam Inc., Cambridge, MA, USA) at room temperature for 30 min. After incubation, the slides were added with diaminobenzidine (DAB) (P0203, Beyotime Institute of Biotechnology, Shanghai, China) for coloration for 5 min at room temperature, followed by 5-min washing under running water, and the degree of coloration was controlled under a microscope. Finally, the slides were counterstained with hematoxylin, differentiated with 1% hydrochloric acid ethanol for 5 s, immersed under running water for 10 min to turn blue, sealed with neutral resin and observed under a microscope. A total of five high-magnification fields were randomly selected from each section, and a total of 100 cells were counted in each field and classified according to the following criteria: the number of positive cells < 10% represented negative; 10% ≤ the number of positive cells < 50% was considered as positive; the number of positive cells ≥ 50% indicated strongly positive [15].

Cell treatment

HTR8/SVneo cells (Shanghai Yubo Biological Technology Co., Ltd., Shanghai, China) were cultured in T25 cell culture flask of 1640 medium (Gibco Company, Grand Island, NY, USA) containing 10% fetal bovine serum (FBS, Gibco Company, Grand Island, NY, USA) at 37 °C in incubator with 5% CO_2 and 20% O_2. When the cell confluence reached 90%, the cells were passaged. The cells were detached with 1 mL of 0.25% trypsin at 37 °C for 2 min, and detachment was terminated with medium containing serum. Then, the collected cells were centrifuged at 800×*g* for 6 min with the supernatant removed, and added with an equal volume of medium containing serum, mixed uniformly and evenly transferred into each cell culture flask.

Hypoxia deoxygenation

When the cell confluence reached approximately 60–80%, the HTR8/Svneo cells were incubated for 2 h in an incubator with 2% O_2, 5% CO_2 and 93% N_2 and then cultured under normal conditions for 6 h. Cells were then transfected with following plasmids: pCMV-HA-null [oe-negative control (NC)], pCMV-HA-NLRP3 (oe-NLRP3), si-scrambled sequence (si-NC), si-NLRP3 interference sequence (si-NLRP3), mimic negative sequence + pCMV-HA-null (mimic-NC + oe-NC), miR-520c-3p sequence + pCMV-HA-null (miR-520c-3p mimic + oe-NC), and miR-520c-3p sequence + pCMV-HA-NLRP3 (miR-520c-3p mimic + oe-NLRP3). The transfection sequences were synthesized by Shanghai Sangon Biotechnology Co., Ltd. (Shanghai, China). The cells were inoculated into a six-well plate 24 h prior to cell transfection. When the cell confluence reached about 50%, the HTR8/Svneo cells were transiently transfected with the above-mentioned sequences via mediation of Lipofectamine 2000 (Invitrogen, Carlsbad, CA, USA) for 6 h, during which, the dosage of plasmid oe-NLRP3 was 2 μg and that of plasmid si-NLRP3 was 100 pmol. After the culture medium was changed, the cells were further cultured for another 48 h and used for subsequent experimentation.

Dual-luciferase reporter gene assay

The bioinformatics prediction website, microRNA.org, was employed to predict the target genes of miR-520c-3p, and then a dual-luciferase reporter gene assay was adopted to further verify whether NLRP3 was a direct target gene of miR-520c-3p. The 3′untranslated region (UTR) gene fragment of NLRP3 was synthesized, and introduced to

the pMIR-reporter vector via the endonuclease sites, *XhoI* and *BamHI*. Then, the mutation site of the complementary sequence of the seed sequence was designed on the NLRP3-3′UTR-wild type (WT). After restriction enzyme digestion, the target fragment was inserted into the pMIR-reporter using T4 DNA ligase. Subsequently, the sequenced correctly luciferase reporter plasmids WT-NLRP3 and mutant (MUT)-NLRP3 were, respectively, co-transfected with miR-520c-3p into the HEK-293T cells (Shanghai Xin Yu Biotech Co., Ltd., Shanghai, China). Following a 48-h period of transfection, the cells were harvested and lysed, followed by centrifugation for 3–5 min with the supernatant collected. The luciferase activity was detected using a dual-luciferase detection kit (RG0005, Beyotime Biotechnology Co., Ltd., Shanghai, China) and a dual-luciferase reporter assay system (Promega, Madison, WI, USA) [16].

Reverse transcription quantitative polymerase chain reaction (RT-qPCR)

An ultra-pure RNA extraction kit (D203-01, Beijing GeneStar Biotechnology Co., Ltd., Beijing, China) was adopted to extract the total RNA. Primers of miR-520c-3p and NLRP3 were designed and then synthesized by Takara Biotechnology Ltd. (Dalian, Liaoning, China), as shown in Table 2. The RNA template, Primer Mix, dNTP Mix, DTT, RT Buffer, HiFi-MMLV and RNase-free water were dissolved on ice for subsequent use. Next, RT-qPCR reaction was carried out according to the manufacture's protocols provided by the TaqMan MicroRNA Assays Reverse Transcription Primer (4366596, Thermo Fisher Scientific, Waltham, MA, USA). The reaction solution was subjected to RT-qPCR in accordance with the instructions of the SYBR® Premix Ex TaqTM II Kit (RR820A, ActionAward Biotechnology Co., Ltd., Guangzhou, Guangdong, China). U6 was used as the internal reference for miR-520c-3p, and glyceraldehyde-3-phosphate dehydrogenase (GAPDH) for NLRP3 (abs830032, Absin Bioscience Inc., Shanghai, China). The fold changes were calculated by means of relative quantification ($2^{-\Delta\Delta Ct}$ method), the formula of which was as follows: $\Delta\Delta Ct = \Delta Ct_{\text{the experimental group}} - \Delta Ct_{\text{the control group}}$, in which $\Delta Ct = Ct_{\text{(target gene)}} - Ct_{\text{(internal reference)}}$. The experiments were repeated three independent times to obtain the mean value.

Table 2 Primer sequences for RT-qPCR

Name	Sequence
miR-520c-3p	F: 5′-GAAGCACTTTCTGTTGTCTGAA-3′
	R: 5′-TCAAACGGTAACCCTCTAAAAGGA-3′
U6	F: 5′-GAATTCCCCAGTGGAAAGACGC-3′
	R: 5′-GGTGTTTCGTCCTTTCCACAAGAT ATATAAAGGG-3′
NLRP3	F: 5′-GGTTTACCAGGGGAAATGAGG-3′
	R: 5′-TTGTGCTTCCAGATGCCGT-3′
GAPDH	F: 5′-ATCACCATCTTCCAGGAGCGA -3′
	R: 5′-GCTTCACCACCTTCTTGATGT-3′

RT-qPCR reverse transcription quantitative polymerase chain reaction, *miR-520c-3p* microRNA-520c-3p, *NLRP3* nod-like receptor pyrin domain-containing 3, *GAPDH* glyceraldehyde-3-phosphate dehydrogenase, *F* forward, *R* reverse

Western blot analysis

The cells at the logarithmic phase of growth were transfected according to cell grouping. Following a 48-h period of transfection, the cell culture medium in the culture flask was removed. Then, the cells were rinsed once with precooled PBS, lysed with radioimmunoprecipitation assay cell lysis buffer on ice for 30 min, followed by centrifugation at 39,451.6×*g* for 10 min. The supernatant was collected for determination of protein concentration using a bicinchoninic acid kit and subsequently preserved at − 20 °C. Next, the proteins were separated by sodium dodecyl sulfate-polyacrylamide gradient gel electrophoresis, and transferred onto a nitrocellulose membrane. The membrane was blocked with 5% bovine serum albumin (BSA) at room temperature for 1 h and then incubated with addition of the following primary antibodies: rabbit polyclonal antibody to NLRP3 (ab214185, dilution ratio of 1:1000), ASC (ab18193, dilution ratio of 1:1000), IL-33 (ab83873, dilution ratio of 1:1000), IL-1β (ab2105, dilution ratio of 1:2000), IL-18 (ab71495, dilution ratio of 1:1000), IL-10 (sc-1783, dilution ratio of 1:1000, Shanghai Univ Biotechnology Co., Ltd., Shanghai, China), caspase-1 (ab62698, dilution ratio of 1:1000), TNF-α (ab6671, dilution ratio of 1:2000), and GAPDH (ab9485, dilution ratio of: 2500) overnight at 4 °C. On the following day, the membrane was washed thrice with polybutylene succinate-co-terephthalate (PBST) (5 min/time) and then incubated with the secondary antibody goat anti-rabbit IgG (ab205718, dilution ratio of 1: 5000) diluted by 5% skim milk powder at room temperature for 1 h on a shaker. All aforementioned antibodies were purchased from Abcam Inc. (Cambridge, MA, USA). After six PBST rinses (5 min/time), the membrane was immersed with a developing agent, and then images were developed using the Bio-Rad gel imaging system (MG8600, Thmorgan Biotechnology Co., Ltd., Beijing, China). The IPP7.0 software (Media Cybernetics, Singapore) was employed for quantitative analysis. At last, the relative protein levels of NLRP3, IL-33, IL-1β, IL-18, IL-10, caspase-1, and TNF-α were expressed as the ratio of the gray value of the target protein bands to that of the GAPDH protein band.

Immunofluorescence assay

The cell slides were treated with poly-L-lysine at room temperature for 1 h, washed thrice with sterilized water (5 min/time), and irradiated using ultraviolet light for 30 min. Then, the cell slides were placed on a 12-well plate and rinsed thrice with PBS. Cell transfection was conducted once the HTR8/Svneo cells adhered to the wall for 24 h. Following a 72-h period of transfection, the cells were rinsed twice with pre-cooled PBS, and fixed in 4% paraformaldehyde for 20 min at room temperature, followed by another three pre-cooled PBS rinses (5 min/time). After rinsing, the cells were blocked with 3% BSA/PBST at room temperature for 1 h, and incubated with 3% BSA/PBST diluted primary antibody overnight at 4 °C. On the following day, the cells were rinsed three times with pre-cooled PBS, and incubated with 3% BSA/PBST diluted secondary antibody for 1 h avoiding exposure to light. After being rinsed thrice with pre-cooled PBS, the cells were incubated with 0.1 μg/mL 4′,6-diamidino-2-phenylindole dihydrochloride for 1 min. Finally, the cells were rinsed three times with pre-cooled PBS, mounted and photographed under a microscope.

Scratch test

The cells were seeded in a six-well plate at a density of 5×10^5 cells/well. Cell transfection was carried out after the cells adhered to the wall. A straight line was scratched on the cell surface using a 200-μL sterile pipette gun and rinsed three times with PBS. Then, the cells were photographed under an inverted microscope at 100× high magnification power (Olympus CX23, Olympus, Tokyo, Japan). After incubation for 48 h, the six-well plate was taken out for photography and scratch rate measurement.

Transwell assay

Matrigel (BD Biosciences, Franklin Lakes, NJ, USA) was diluted with pre-cooled serum-free Dulbecco's modified Eagle medium (DMEM) at a ratio of 1:10. The apical chamber was washed with 200 μL of serum-free 1640 medium, and then added with 100 μL of diluted Matrigel, which was then placed at room temperature for 2 h. Following a 24-h period of transfection, the cells were detached, resuspended in serum-free DMEM medium, counted and diluted to a cell density of 3×10^5 cells/μL. Next, 100 μL of cells were added to the apical chamber of transwell chamber (Corning Glass Works, Corning, NY, USA), and 600 μL of DMEM medium containing 10% serum was added to the basolateral chamber. According to the instructions of the transwell assay kit, the cells were stained with crystal violet and three view fields were randomly selected to count the number of invasive cells.

Statistical analysis

SPSS 21.0 statistical software (IBM Corp. Armonk, NY, USA) was employed to analyze the data, which were processed with normal distribution and homogeneity of variance. Data in accordance with normal distribution were expressed as mean ± standard deviation; those inconsistent with normal distribution or homogeneity of variance were presented by interquartile range. Comparisons between two groups were analyzed using the *t* test, and data with skewed distribution were analyzed by nonparametric Wilcoxon signed rank test. Comparisons among multiple groups were assessed by one-way analysis of variance (ANOVA). A value of $p<0.05$ was considered to be statistically significant.

Results

Imbalanced levels of inflammatory cytokines and upregulated levels of NLRP3 are observed in PE placenta tissues

Initially, we performed ELISA to determine the levels of IL-18, IL-33, IL-1β, IL-10, and TNF-α in normal and PE placenta tissues. As shown in Fig. 1a, significantly upregulated levels of IL-18, IL-1β, and TNF-α, while downregulated IL-10 and IL-33 were noted in the PE placenta tissues when compared with the normal placenta tissues ($p<0.05$). These findings illustrated that the levels of inflammatory cytokines were aberrantly expressed in PE placenta tissues.

Similarly, increased levels of NLRP3 in PE placenta tissues were previously demonstrated and suggested to be involved in severe inflammation in PE [8]. Thus, RT-qPCR and immunohistochemistry were performed to further verify the expression patterns of NLRP3. The positive protein levels of NLRP3 were primarily expressed in the cytoplasm and observed as light yellow, yellowish-brown, or tan coloration. Compared with the normal placenta tissues, the PE placenta tissues exhibited markedly elevated positive protein levels of NLRP3 ($p<0.05$) (Fig. 1b, c). These results suggested that NLRP3 is upregulated in the pathogenesis of PE.

NLRP3 inhibits the inflammatory cascade in HTR8/SVneo cells after hypoxia and enhances cell migration and invasion

Aiming to investigate whether NLRP3 could initiate the inflammatory cascade in PE, first, we detected the expression of NLRP3 in control HTR8/SVneo cells without any treatment and HTR8/SVneo cells treated with hypoxia. As shown in Fig. 2a, NLRP3 expression was considerably higher in HTR8/SVneo cells treated with hypoxia than that in control HTR8/SVneo cells without any treatment.

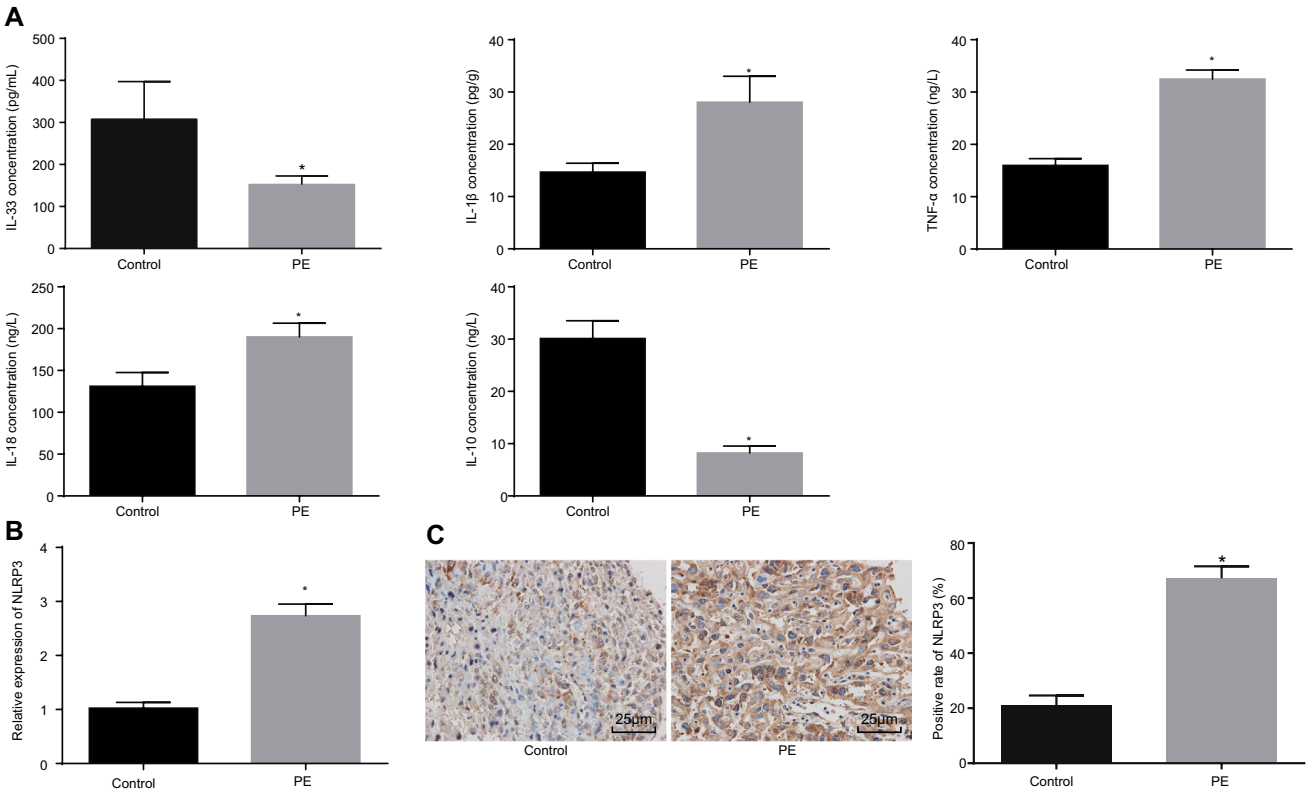

Fig. 1 Imbalanced levels of inflammatory cytokines and upregulated levels of NLRP3 in PE placenta tissues. **a** The levels of IL-18, IL-33, IL-10, IL-1β, and TNF-α in PE and normal placenta tissues detected by ELISA; **b** the expression patterns of NLRP3 in PE and normal placenta tissues measured by RT-qPCR; **c** the positive protein levels of NLRP3 in PE and normal placenta tissues determined by immunohistochemistry (×400); $*p < 0.05$ vs. the control group; the data were analyzed by independent sample *t* test; $N = 30$. *PE* preeclampsia, *NLRP3* nod-like receptor pyrin domain-containing 3, *IL* interleukin, *TNF-α* tumor necrosis factor α, *RT-qPCR* reverse transcription quantitative polymerase chain reaction, *ELISA* enzyme-linked immunosorbent assay

Next, hypoxic HTR8/SVneo cells were transfected with oe-NLRP3 or si-NLRP3. Then, the protein levels of NLRP3 inflammasomes (NLRP3, ASC, and caspase-1) were detected by means of western blot analysis, wherein caspase-1 activity was also measured using an ELISA kit; the levels of IL-18, IL-33, IL-1β, and TNF-α that followed in HTR8/SVneo cells after hypoxia were determined by western blot analysis, wherein IL-1β levels were also evaluated by immunofluorescence assay (Fig. 2e, f). Additionally, the cell migration and invasion abilities were assessed using scratch tests and transwell assay. The results revealed that HTR8/SVneo cells after hypoxia transfected with si-NLRP3 exhibited decreased levels of NLRP3, ASC, and caspase-1 (Fig. 2b, c), significantly suppressed caspase-1 activity (Fig. 2d), in addition to evidently downregulated protein levels of IL-18, IL-1β, and TNF-α, upregulated protein levels of IL-10 and IL-33 (Fig. 2g, h), and enhanced cell invasion and migration abilities (Fig. 2i–l) (all $p < 0.05$). However, entirely opposite tendencies were noted in the cells transfected with oe-NLRP3 (all $p < 0.05$). Altogether, these findings demonstrated that silencing of NLRP3 could inhibit activation of the NLRP3 inflammasome, while suppressing the inflammatory cascade in HTR8/SVneo cells after hypoxia and enhancing cell migration and invasion.

NLRP3 is a target gene of miR-520c-3p

To explore the upstream regulators of NLRP3, we predicted the miRNA with the potential to regulate NLRP3 using the TargetScan (http://www.targetscan.org/vert_71/) database and DIANA TOOLS (http://diana.imis.athena-innovation.gr/DianaTools/index.php?r=site/page&view=software) and the PE-related dataset GSE96983. The results revealed the presence of a specific binding site between the NLRP3 gene sequence and miR-520c-3p (Fig. 3a–c). Hypoxia was suggested to be a risk factor for PE due to its ability to inhibit the differentiation of trophoblastic cells [17]. Furthermore, an enriched expression of miR-520c-3p has been previously found in trophoblastic cells, following its downregulation after hypoxia treatment [13]. Therefore, we speculated that miR-520c-3p targeting NLRP3 might be involved in the initiation of PE. Subsequently, a dual-luciferase reporter gene

assay was adopted to further verify the targeting relationship between miR-520c-3p and NLRP3. The results demonstrated that cells transfected with miR-520c-3p mimic showed decreased luciferase activity of NLRP3-3′UTR-WT compared to HEK-293T cells transfected with mimic-NC ($p < 0.05$), while those of NLRP3-3′UTR-MUT displayed no significant changes ($p > 0.05$) (Fig. 3d). Furthermore, miR-520c-3p expression in PE and normal placenta tissues was evaluated by RT-qPCR, the results of which showed that PE placenta tissues exhibited significantly decreased expression of miR-520c-3p compared to normal placenta tissues ($p < 0.05$) (Fig. 3e). All these results demonstrated that miR-520c-3p could specifically bind to the NLRP3-3′UTR, and was expressed at a low level in PE placenta tissues.

miR-520c-3p inhibits NLRP3 inflammasome activation and inflammatory cascade in HTR8/SVneo cells after hypoxia by downregulating NLRP3

To investigate whether miR-520c-3p targeting NLRP3 affected inflammatory cascade in PE, we detected the expression of miR-520c-3p in control HTR8/SVneo cells without any treatment and HTR8/SVneo cells treated with hypoxia, as well as the protein expression of downstream inflammatory factors (IL-1β, TNF-α and IL-18) by means of western blot analysis. The results showed that the expression of miR-520c-3p in hypoxic HTR8/SVneo cells was significantly lower than that in the control HTR8/SVneo cells (Fig. 4a). Meanwhile, western blot analysis results revealed that the protein expression of IL-1β, TNF-α and IL-18 in hypoxic HTR8/SVneo cells was significantly elevated, while that of IL-33 and IL-10 was evidently reduced in hypoxic HTR8/SVneo cells (Fig. 4b, c).

Subsequently, hypoxic HTR8/SVneo cells were transfected with miR-520c-3p mimic and miR-520c-3p mimic + oe-NLRP3, followed by evaluation of the levels of NLRP3 inflammasomes and inflammatory cytokines. Compared with the mimic NC + oe-NC group, the hypoxic HTR8/SVneo cells following transfection with miR-520c-3p mimic and oe-NC were noted to exhibit decreased protein levels of NLRP3, ASC, and caspase-1 (Fig. 4a, b) and a declined caspase-1 activity (Fig. 4c), in addition to downregulated levels of IL-1β, TNF-α and IL-18, while those of IL-10 and IL-33, were upregulated (Fig. 4d) ($p < 0.05$). However, opposite trends were noted in hypoxic HTR8/SVneo cells transfected with miR-520c-3p mimic + oe-NLRP3 when compared to those transfected with miR-520c-3p mimic + oe-NC (all $p < 0.05$). Together, these results evidenced that overexpression of miR-520c-3p was capable of inhibiting NLRP3 inflammasome activation and suppressing inflammatory cascade in HTR8/SVneo cells after hypoxia through downregulation of NLRP3.

Discussion

A maternal systemic inflammatory response is a commonly occurring phenomenon in normal pregnancy but is known to be enhanced in the presence of PE [18]. Inflammatory changes in early-staged pregnancy have been previously hypothesized to be contributors of coagulation system activation and cell death induction, leading to impaired placental invasion in women with PE [19]. In addition, the activation of NLRP3 inflammasome in trophoblasts has been suggested to elevate IL-1β levels in the placenta and lead to PE pathogenesis [20]. A former study further implied that miR-223 could suppress the expression of NLRP3 via a conserved binding site within the NLRP3-3′-UTR, thus translating to reduced activity of the NLRP3 inflammasome [21]. In the current study, we explored the underlying role of miR-520c-3p in the inflammation cascade of PE. Collectively, the experimental data revealed that overexpression of miR-520c-3p impedes the activation of the NLRP3 inflammasome and inflammation cascade in PE via downregulation of NLRP3.

First, we uncovered that PE placenta tissues exhibited upregulated levels of IL-18, IL-1β, and TNF-α and downregulated levels of IL-10 and IL-33. The release of IL-33 is habitually noted once the epithelium and endothelium receive inflammatory signals or undergo necrosis [22]. Similarly, a previously study also demonstrated reduced levels of IL-33 in PE placenta tissues, and further revealed that trophoblast cells introduced with IL-33 shRNA presented with significantly attenuated capacities of proliferation, migration, and invasion [23]. PE is linked to an integral pro-inflammatory systemic environment, which is demonstrated by circulating factors derived from placentas to promote pro-inflammatory cell production of cytokines such as IL-1β, IL-10, IL-18, and TNF-α [24]. Insufficient trophoblast invasion and failed placental spiral artery remolding in PE result in poor placentation, stimulated IL-β production and, in turn, over-production of inflammatory cytokines (TNF-α) [25]. In addition, IL-18 has been proposed to play vital roles in pregnancy, labor onset and pregnant complications, and elevated levels of IL-18 in serum and placenta have been previously evidenced in PE [26]. Moreover, an inflammatory environment induced by hypoxia accompanied by IL-10 deficiency was previously suggested to influence trophoblast functions and disturb maternal-fetal interface apoptosis-associated pathways [27]. Additionally, a previous study verified the existence of unbalanced inflammatory cytokine production of pro-inflammatory cytokines (TNF-α) and anti-inflammatory cytokines (IL-10) in the placental-decidual interface [6]. These findings and results point towards the involvement of imbalanced inflammatory cytokine production in PE.

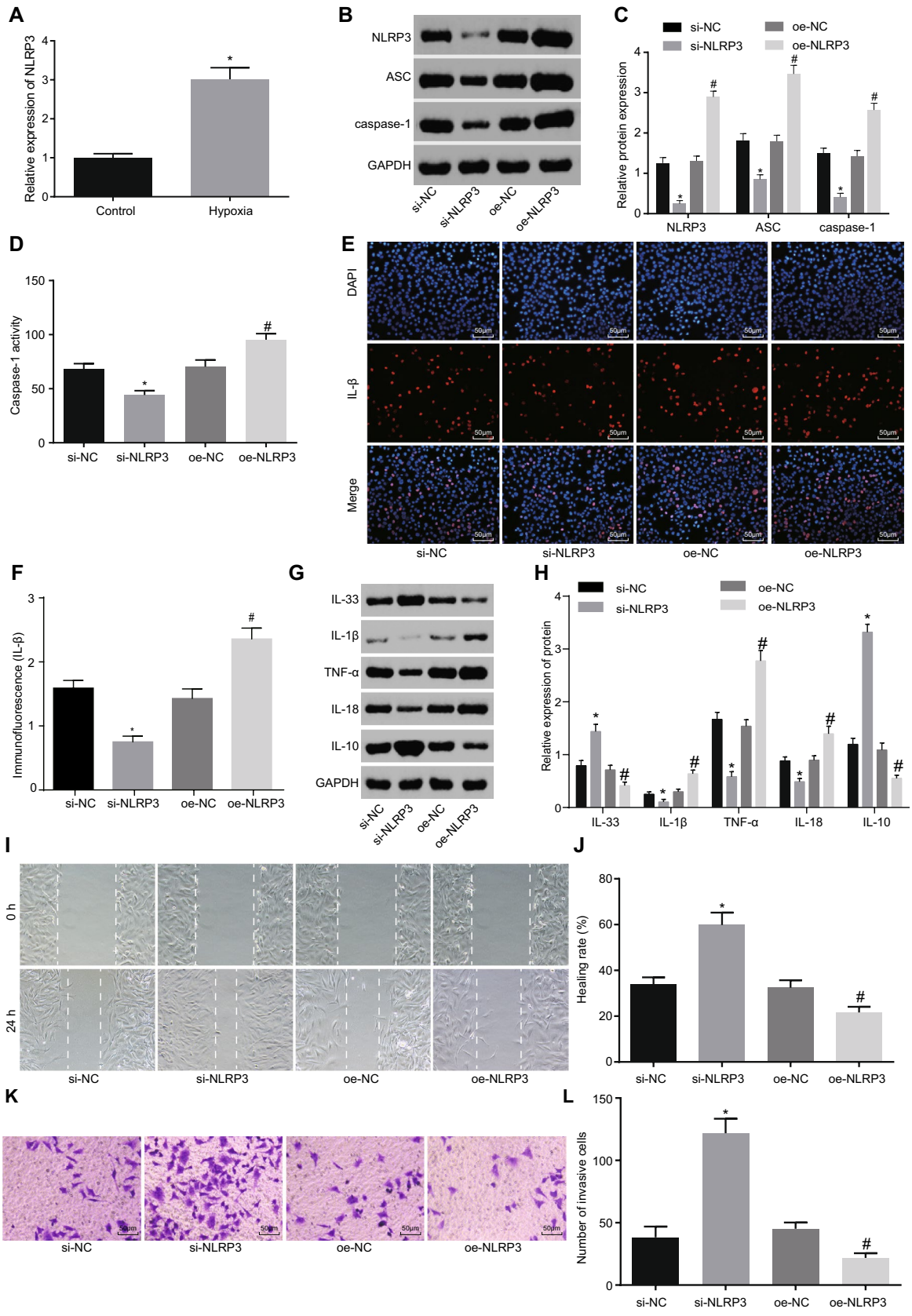
A
Relative expression of NLRP3
Control
Hypoxia
B
NLRP3
ASC
caspase-1
GAPDH
si-NC
si-NLRP3
oe-NC
oe-NLRP3
C
si-NC
si-NLRP3
oe-NC
oe-NLRP3
Relative protein expression
NLRP3
ASC
caspase-1
D
Caspase-1 activity
si-NC
si-NLRP3
oe-NC
oe-NLRP3
E
DAPI
IL-β
Merge
50μm
si-NC
si-NLRP3
oe-NC
oe-NLRP3
F
Immunofluorescence (IL-β)
si-NC
si-NLRP3
oe-NC
oe-NLRP3
G
IL-33
IL-1β
TNF-α
IL-18
IL-10
GAPDH
si-NC
si-NLRP3
oe-NC
oe-NLRP3
H
si-NC
si-NLRP3
oe-NC
oe-NLRP3
Relative expression of protein
IL-33
IL-1β
TNF-α
IL-18
IL-10
I
0 h
24 h
si-NC
si-NLRP3
oe-NC
oe-NLRP3
J
Healing rate (%)
si-NC
si-NLRP3
oe-NC
oe-NLRP3
K
50μm
si-NC
si-NLRP3
oe-NC
oe-NLRP3
L
Number of invasive cells
si-NC
si-NLRP3
oe-NC
oe-NLRP3

◂**Fig. 2** Suppression of NLRP3 inflammasomes and inflammatory cascade activation in HTR8/SVneo cells after hypoxia by silencing NLRP3. **a** mRNA expression patterns of NLRP3 in HTR8/SVneo cells in the control and hypoxia groups determined by RT-qPCR; **b**, **c** western blot analysis of NLRP3 inflammasomes (NLRP3, ASC, and caspase-1) protein levels in hypoxic HTR8/SVneo cells following transfection of si-NLRP3 and oe-NLRP3; **d** the activity of caspase-1 in hypoxic HTR8/SVneo cells following transfection of si-NLRP3 and oe-NLRP3 detected by caspase-1 ELISA kit; **e**, **f** immunofluorescence analysis of IL-1β protein levels in hypoxic HTR8/SVneo cells following transfection of si-NLRP3 and oe-NLRP3 (×200); **g**, **h** western blot analysis of IL-18, IL-33, IL-10, IL-1β, and TNF-α protein levels in hypoxic HTR8/SVneo cells following transfection of si-NLRP3 and oe-NLRP3; **i**, **g** cell migration of hypoxic HTR8/SVneo cells following transfection of si-NLRP3 and oe-NLRP3 assessed by scratch test (×100); **k**, **l** cell invasion of hypoxic HTR8/SVneo cells following transfection of si-NLRP3 and oe-NLRP3 determined by transwell assay (×200); $^{*}p<0.05$ vs. the si-NC group or the control group; $^{\#}p<0.05$ vs. the oe-NC group; the data were analyzed by the independent sample *t* test; the experiments were independently repeated three times. *NLRP3* nod-like receptor pyrin domain-containing 3, *ASC* apoptosis-associated speck-like protein containing a CARD, *IL* interleukin, *TNF-α* tumor necrosis factor α, *ELISA* enzyme-linked immunosorbent assay, *NC* negative control, *GAPDH* glyceraldehyde-3-phosphate dehydrogenase

NLRP3 was demonstrated in this study to be expressed at a high level in PE placenta tissues. We further discovered that cells after transfection with si-NLRP3 presented with significantly reduced levels of IL-1β, IL-18, and TNF-α and NLRP3 inflammasomes (NLRP3, ASC and caspase-1), in addition to enhanced migration and invasion abilities and increased IL-10 and IL-33 levels by investigating the effects of NLRP3 silencing on the HTR8/Svneo cells after hypoxia. In line with our findings, a previous study also verified that expression of NLRP3 inflammasomes is upregulated in PE placentas, revealing a bridge that links aggravated inflammatory state and activated NLRP3 inflammasomes [8]. In addition, as a major component of the NLRP3 inflammasomes, silencing of NLRP3 has been suggested to lead to enhanced NLRP3 inflammasome activity [9]. Similarly, a previous study proposed that knockdown of NLRP3 represses the production of pro-inflammatory and pro-labor mediators induced by inflammation in human myometrium [28]. As a type of multiprotein complexes, NLRP3 inflammasomes can further activate caspase-1 to drive the processing and secretion of the pro-inflammatory cytokines IL-1β and IL-18 [29]. NLRP3 inflammasomes comprise ASC and pro-caspase-1, wherein ASC recruitment partially resulting from NLRP3 inflammasome activation can in turn induce the caspase-1 autocatalytic activation, and then produce p10 and p20 caspase-1 trigger bioactive and secreted forms of inactive pro-IL-1β and pro-IL-18 as a result of the formation of active caspase-1 hetero-tetramers [30]. Furthermore, the activation of NLRP3 inflammasome is known to be involved in the inflammatory response and cell death in hypoxia-induced β-cells through the ROS–TXNIP–NLRP3 axis in vitro, ultimately potentiating the release of downstream inflammatory factors, such as IL-1β and IL-6 [31]. Based on the above analysis, we reached a conclusion that NLRP3 silencing could inhibit the activation of NLRP3 inflammasomes to alleviate the inflammatory cascade in PE.

Additionally, we discovered that miR-520c-3p was downregulated in PE placenta tissues, suggesting that miR-520c-3p functions as a negative regulator of NLRP3. Moreover, HTR8/Svneo cells after hypoxia with delivery of miR-520c-3p mimic exhibited reduced levels of IL-1β, IL-18, and TNF-α and NLRP3 inflammasomes, and elevated levels of IL-10 and IL-33 as well as promoted cell migration and invasion abilities. In line with our findings, a previous study illustrated that expression of miRNAs is downregulated in PE placenta tissues, especially that of miR-454, which is implicated in the facilitation of trophoblast cell abilities of proliferation and invasion while attenuating apoptosis by inhibiting the expression of the ephrin receptor B4 [32]. Furthermore, reduced expression of miR-146a and miR-155 has been observed in syncytiotrophoblast of the intermediate villi and syncytial knots in late-onset PE relative to full-term physiological pregnancy [33]. Hypoxia is known to contribute to limited trophoblast differentiation [17], and was also previously demonstrated to decrease the expression of miR-520c-3p which is enriched in trophoblasts [13]. Extravillous trophoblast exosomal miR-520c-3p targeted CD44 is indicated to modulate extravillous trophoblast invasion [34]. Moreover, a previous study reported that miR-9 is capable of inhibiting the activation of NLRP3 inflammasome to attenuate inflammation in atherosclerosis possibly via the Janus kinase 1/signal transducers and activators of the transcription 1 pathway [35]. The above-mentioned results suggest that overexpression of miR-520c-3p can inhibit the activation of NLRP3 inflammasomes by downregulating NLRP3, leading to the suppression of the inflammatory cascade in HTR8/SVneo cells after hypoxia.

Conclusions

In conclusion, findings of the current study suggest that miR-520c-3p may serve as a potential therapeutic target for PE treatment in the future as miR-520c-3p disrupts the activation of the NLRP3 inflammasome activation and inflammation cascade while promoting cell invasion and proliferation through downregulation of NLRP3. Therefore, future studies with larger sample sizes involving human populations are warranted to efficiently utilize miR-targeted therapy for PE.

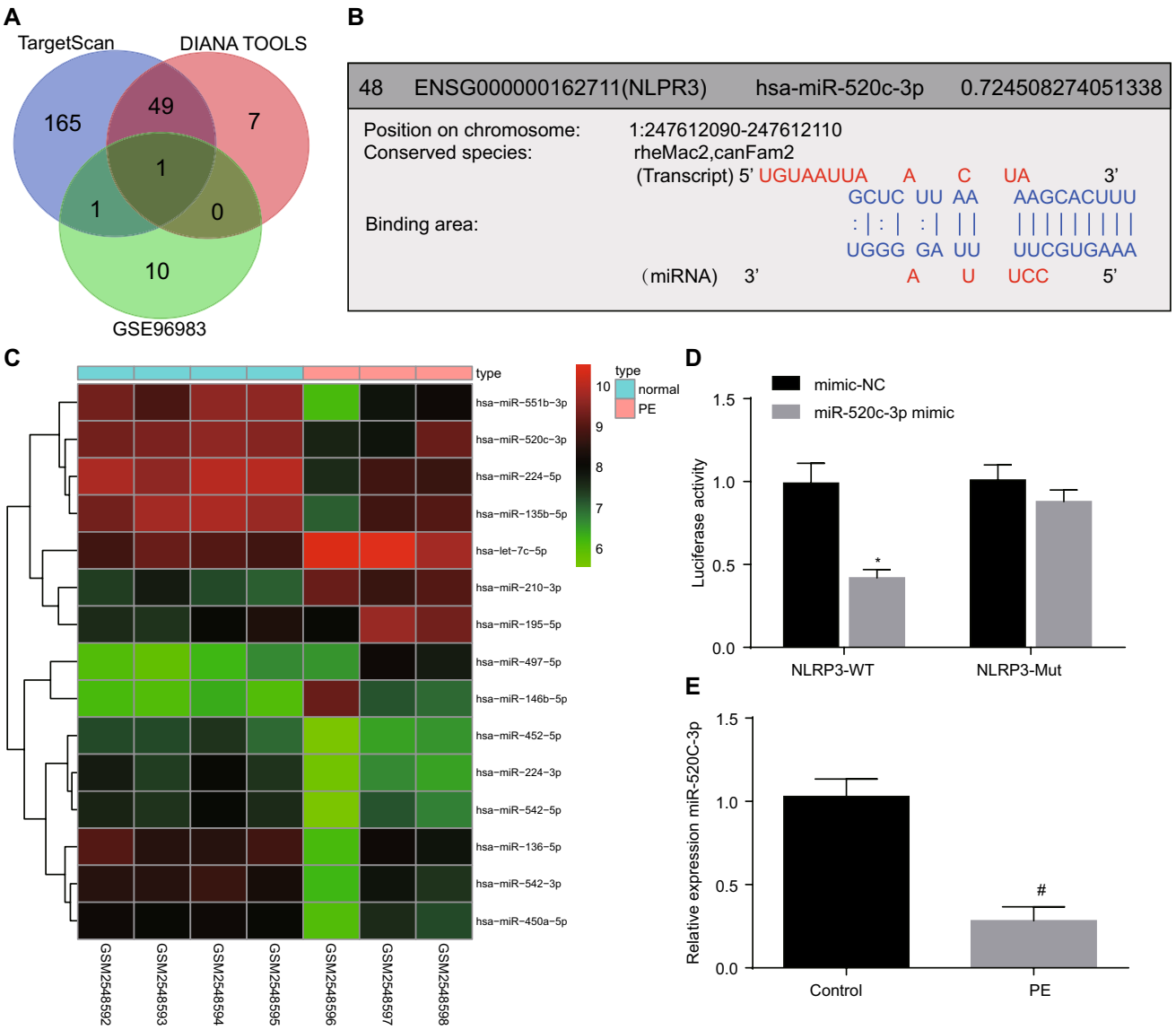

Fig. 3 NLRP3 is a target gene of miR-520c-3p. **a** The screened miRNA with the potential to regulate NLRP3 through TargetScan; **b** the predicted binding site between NLRP3 gene sequence and miR-520c-3p through DIANA TOOLS; **c** the heat map of differentially expressed genes screened from the GSE96983 datasets; the abscissa represents the sample number, and the coordinate represents the gene items; the histogram in the upper right represents the color gradation, and each rectangle corresponds to one gene expression in one sample; **d** the luciferase activity of NLRP3-3′UTR-WT/MUT after transfection with miR-520c-3p mimic or mimic NC determined by dual-luciferase reporter gene assay; **e** the miR-520c-3p expression in PE and normal placenta tissues assessed by RT-qPCR; $^{*}p < 0.05$ vs. the mimic-NC group; $^{\#}p < 0.05$ vs. the control group; the data were analyzed by the independent sample *t* test; the experiments were independently repeated three times. *PE* preeclampsia, *miR-520c-3p* microRNA-520c-3p, *NLRP3* nod-like receptor pyrin domain-containing 3, *RT-qPCR* reverse transcription quantitative polymerase chain reaction, *WT* wild type, *MUT* mutant, *UTR* untranslated region, *NC* negative control

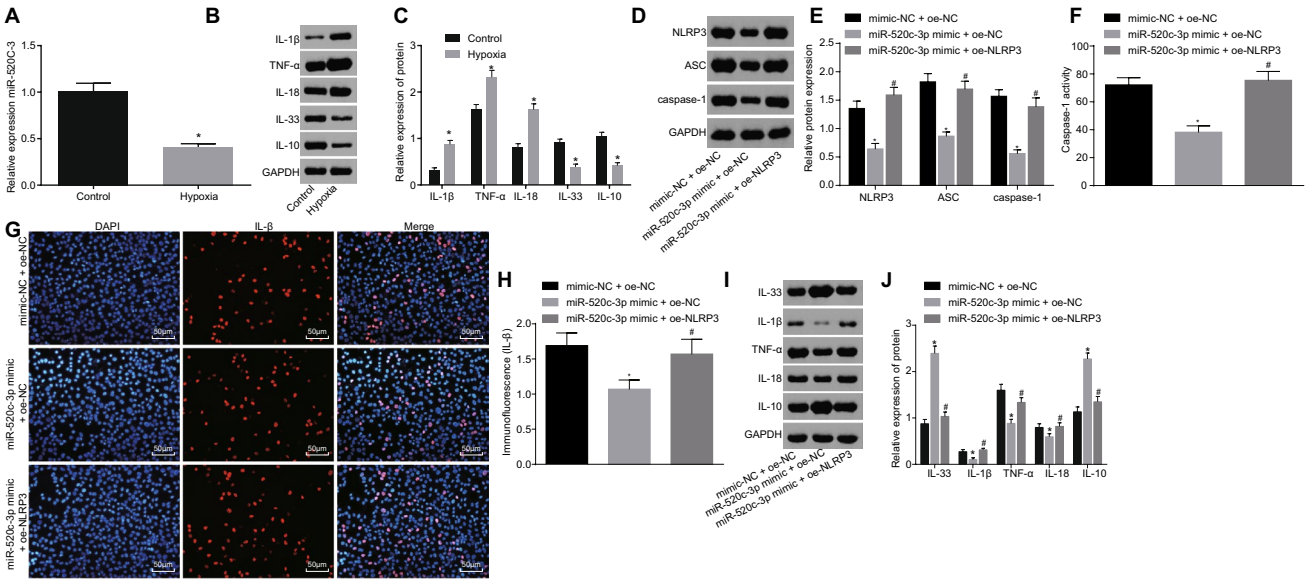

Fig. 4 miR-520c-3p inactivates NLRP3 inflammasomes through downregulation of NLRP3, thereby inhibiting inflammatory cascade in HTR8/SVneo cells after hypoxia. **a** Expression patterns of miR-520c-3p in HTR8/SVneo cells in the control and hypoxia groups determined by RT-qPCR; **b**, **c** western blot analysis of IL-1β, TNF-α and IL-18 protein levels in HTR8/SVneo cells following transfection of miR-520c-3p mimic and miR-520c-3p mimic + oe-NLRP3; **d**, **e** western blot analysis of NLRP3 inflammasomes (NLRP3, ASC, and caspase-1) protein levels in HTR8/SVneo cells following transfection of miR-520c-3p mimic and miR-520c-3p mimic + oe-NLRP3; **f** the activity of caspase-1 in cells following transfection of miR-520c-3p mimic and miR-520c-3p mimic + oe-NLRP3 detected by caspase-1 ELISA kit; **g**, **h** Immunofluorescence analysis of IL-1β in cells following transfection of miR-520c-3p mimic and miR-520c-3p mimic + oe-NLRP3 (×200); **i**, **j** western blot analysis of IL-18, IL-33, IL-10, IL-1β, and TNF-α protein levels following transfection of miR-520c-3p mimic and miR-520c-3p mimic + oe-NLRP3; $^{*}p < 0.05$ vs. the si-NC group or the control group; $^{\#}p < 0.05$ vs. the miR-520c-3p mimic + oe-NC group; the data were analyzed by the independent sample *t* test; the experiments were independently repeated three times. *miR-520c-3p* microRNA-520c-3p, *NLRP3* nod-like receptor pyrin domain-containing 3, *ASC* apoptosis-associated speck-like protein containing a CARD, *IL* interleukin, *TNF-α* tumor necrosis factor α, *ELISA* enzyme-linked immunosorbent assay, *NC* negative control, *GAPDH* glyceraldehyde-3-phosphate dehydrogenase

Acknowledgements We would like show sincere appreciation to the reviewers for critical comments on this article.

Compliance with ethical standards

Conflict of interest The authors' declares that they have no conflict of interest.

References

1. Kohli S, Ranjan S, Hoffmann J, Kashif M, Daniel EA, Al-Dabet MM, et al. Maternal extracellular vesicles and platelets promote preeclampsia via inflammasome activation in trophoblasts. Blood. 2016;128:2153–64.
2. Leavey K, Benton SJ, Grynspan D, Kingdom JC, Bainbridge SA, Cox BJ. Unsupervised placental gene expression profiling identifies clinically relevant subclasses of human preeclampsia. Hypertension. 2016;68:137–47.
3. Brien ME, Boufaied I, Soglio DD, Rey E, Leduc L, Girard S. Distinct inflammatory profile in preeclampsia and postpartum preeclampsia reveal unique mechanisms. Biol Reprod. 2018;100(1):187–94.
4. Winship A, Dimitriadis E. Interleukin 11 is upregulated in preeclampsia and leads to inflammation and preeclampsia features in mice. J Reprod Immunol. 2018;125:32–8.
5. Harmon AC, Cornelius DC, Amaral LM, Faulkner JL, Cunningham MW Jr, Wallace K, et al. The role of inflammation in the pathology of preeclampsia. Clin Sci (Lond). 2016;130:409–19.
6. Valencia-Ortega J, Zarate A, Saucedo R, Hernandez-Valencia M, Cruz JG, Puello E. Placental proinflammatory state and maternal endothelial dysfunction in preeclampsia. Gynecol Obstet Invest. 2018;84(1):12–9.
7. Yin Y, Zhou Z, Liu W, Chang Q, Sun G, Dai Y. Vascular endothelial cells senescence is associated with NOD-like receptor family pyrin domain-containing 3 (NLRP3) inflammasome activation via reactive oxygen species (ROS)/thioredoxin-interacting protein (TXNIP) pathway. Int J Biochem Cell Biol. 2017;84:22–34.
8. Weel IC, Romao-Veiga M, Matias ML, Fioratti EG, Peracoli JC, Borges VT, et al. Increased expression of NLRP3 inflammasome in placentas from pregnant women with severe preeclampsia. J Reprod Immunol. 2017;123:40–7.
9. Hu J, Zhu Y, Zhang JZ, Zhang RG, Li HM. A novel mutation in the pyrin domain of the NOD-like receptor family pyrin domain containing protein 3 in Muckle-Wells syndrome. Chin Med J (Engl). 2017;130:586–93.
10. Wang Y, Dong Q, Gu Y, Groome LJ. Up-regulation of miR-203 expression induces endothelial inflammatory response: potential role in preeclampsia. Am J Reprod Immunol. 2016;76:482–90.

11. Keklikoglou I, Koerner C, Schmidt C, Zhang JD, Heckmann D, Shavinskaya A, et al. MicroRNA-520/373 family functions as a tumor suppressor in estrogen receptor negative breast cancer by targeting NF-kappaB and TGF-beta signaling pathways. Oncogene. 2012;31:4150–63.
12. Lee YH, Na HS, Jeong SY, Jeong SH, Park HR, Chung J. Comparison of inflammatory microRNA expression in healthy and periodontitis tissues. Biocell. 2011;35:43–9.
13. Donker RB, Mouillet JF, Chu T, Hubel CA, Stolz DB, Morelli AE, et al. The expression profile of C19MC microRNAs in primary human trophoblast cells and exosomes. Mol Hum Reprod. 2012;18:417–24.
14. Zhou R, Tardivel A, Thorens B, Choi I, Tschopp J. Thioredoxin-interacting protein links oxidative stress to inflammasome activation. Nat Immunol. 2010;11:136–40.
15. Atkins D, Reiffen KA, Tegtmeier CL, Winther H, Bonato MS, Storkel S. Immunohistochemical detection of EGFR in paraffin-embedded tumor tissues: variation in staining intensity due to choice of fixative and storage time of tissue sections. J Histochem Cytochem. 2004;52:893–901.
16. Wang B, Shen ZL, Gao ZD, Zhao G, Wang CY, Yang Y, et al. MiR-194, commonly repressed in colorectal cancer, suppresses tumor growth by regulating the MAP4K4/c-Jun/MDM2 signaling pathway. Cell Cycle. 2015;14:1046–58.
17. Hardy DB, Yang K. The expression of 11 beta-hydroxysteroid dehydrogenase type 2 is induced during trophoblast differentiation: effects of hypoxia. J Clin Endocrinol Metab. 2002;87:3696–701.
18. Staff AC, Johnsen GM, Dechend R, Redman CWG. Preeclampsia and uteroplacental acute atherosis: immune and inflammatory factors. J Reprod Immunol. 2014;101–102:120–6.
19. Kwaan HC, Wang J, Boggio L, Weiss I, Grobman WA. The thrombogenic effect of an inflammatory cytokine on trophoblasts from women with preeclampsia. Am J Obstet Gynecol. 2004;191:2142–7.
20. Matias ML, Romao M, Weel IC, Ribeiro VR, Nunes PR, Borges VT, et al. Endogenous and uric acid-induced activation of nlrp3 inflammasome in pregnant women with preeclampsia. PLoS One. 2015;10:e0129095.
21. Bauernfeind F, Rieger A, Schildberg FA, Knolle PA, Schmid-Burgk JL, Hornung V. NLRP3 inflammasome activity is negatively controlled by miR-223. J Immunol. 2012;189:4175–81.
22. Qiu C, Li Y, Li M, Li M, Liu X, McSharry C, et al. Anti-interleukin-33 inhibits cigarette smoke-induced lung inflammation in mice. Immunology. 2013;138:76–82.
23. Chen H, Zhou X, Han TL, Baker PN, Qi H, Zhang H. Decreased IL-33 production contributes to trophoblast cell dysfunction in pregnancies with preeclampsia. Mediat Inflamm. 2018;2018:9787239.
24. Naruse K, Akasaka J, Shigemitsu A, Tsunemi T, Koike N, Yoshimoto C, et al. Involvement of visceral adipose tissue in immunological modulation of inflammatory cascade in preeclampsia. Mediat Inflamm. 2015;2015:325932.
25. Xie C, Yao MZ, Liu JB, Xiong LK. A meta-analysis of tumor necrosis factor-alpha, interleukin-6, and interleukin-10 in preeclampsia. Cytokine. 2011;56:550–9.
26. Huang X, Huang H, Dong M, Yao Q, Wang H. Serum and placental interleukin-18 are elevated in preeclampsia. J Reprod Immunol. 2005;65:77–87.
27. Lai Z, Kalkunte S, Sharma S. A critical role of interleukin-10 in modulating hypoxia-induced preeclampsia-like disease in mice. Hypertension. 2011;57:505–14.
28. Lim R, Lappas M. NOD-like receptor pyrin domain-containing-3 (NLRP3) regulates inflammation-induced pro-labor mediators in human myometrial cells. Am J Reprod Immunol. 2018;79:e12825.
29. Tschopp J, Schroder K. NLRP3 inflammasome activation: the convergence of multiple signalling pathways on ROS production? Nat Rev Immunol. 2010;10:210–5.
30. De Nardo D, Latz E. NLRP3 inflammasomes link inflammation and metabolic disease. Trends Immunol. 2011;32:373–9.
31. Chen C, Ma X, Yang C, Nie W, Zhang J, Li H, et al. Hypoxia potentiates LPS-induced inflammatory response and increases cell death by promoting NLRP3 inflammasome activation in pancreatic beta cells. Biochem Biophys Res Commun. 2018;495:2512–8.
32. Wang F, Yan J. MicroRNA-454 is involved in regulating trophoblast cell proliferation, apoptosis, and invasion in preeclampsia by modulating the expression of ephrin receptor B4. Biomed Pharmacother. 2018;107:746–53.
33. Nizyaeva NV, Kulikova GV, Nagovitsyna MN, Kan NE, Prozorovskaya KN, Shchegolev AI, et al. Expression of microRNA-146a and microRNA-155 in placental villi in early- and late-onset preeclampsia. Bull Exp Biol Med. 2017;163:394–9.
34. Takahashi H, Ohkuchi A, Kuwata T, Usui R, Baba Y, Suzuki H, et al. Endogenous and exogenous miR-520c-3p modulates CD44-mediated extravillous trophoblast invasion. Placenta. 2017;50:25–31.
35. Wang Y, Han Z, Fan Y, Zhang J, Chen K, Gao L, et al. MicroRNA-9 inhibits NLRP3 inflammasome activation in human atherosclerosis inflammation cell models through the JAK1/STAT signaling pathway. Cell Physiol Biochem. 2017;41:1555–71.